Desalination and Water Treatment
www.deswater.com

doi: 10.5004/dwt.2017.20146

62 (2017) 457–464
February

Synergy between solar photocatalysis and high frequency sonolysis toward the degradation of organic pollutants in aqueous phase – case of phenol

Salim Bekkouche[a], Mohamed Bouhelassa[a], Akila Ben Aissa[a], Stéphane Baup[b], Nicolas Gondrexon[b], Christian Pétrier[b], Slimane Merouani[a], Oualid Hamdaoui[c,*]

[a]*Laboratory of Environmental Process Engineering, Department of Process Engineering, Faculty of Process Engineering, University of Constantine 3, 25000 Constantine, Algeria, emails: salim_chim@yahoo.fr (S. Bekkouche), mbouhela@hotmail.com (M. Bouhelassa), akilabenaissa@yahoo.fr (A.B. Aissa), s.merouani@yahoo.fr (S. Merouani)*
[b]*Laboratoire Rhéologie et Procédés, Université Joseph Fourier, 38041 Grenoble cedex 9, France, emails: baup@ujf-grenoble.fr (S. Baup), nicolas.gondrexon@ujf-grenoble.fr (N. Gondrexon), christian.petrier@lepmi.inpg.fr (C. Pétrier)*
[c]*Laboratory of Environmental Engineering, Department of Process Engineering, Faculty of Engineering, Badji Mokhtar – Annaba University, 23000 Annaba, Algeria, Tel./Fax: +213 38876560; emails: ohamdaoui@yahoo.fr, oualid.hamdaoui1@gmail.com*

Received 30 May 2016; Accepted 4 August 2016

ABSTRACT

The degradation of phenol, as an organic pollutant model, in water was systematically assessed under solar TiO_2-photocatalysis in forced circulation loop reactor. The degradation rate was evaluated at various amounts of TiO_2 and different initial concentrations of phenol. Additionally, the influence of coupling heterogeneous photocatalysis with high frequency ultrasonic irradiation (600 kHz) was investigated at various initial substrate concentrations. For both processes, •OH radical was the main species responsible for the oxidation of phenol. The photocatalytic degradation rate of phenol increased with increasing TiO_2 concentration up to 1 g L^{-1} and decreased afterward. The solar photocatalytic process is efficient even if the pollutant exists at high concentration levels. The initial degradation rate increased with increasing initial substrate concentration, following a complex kinetics that was found to be perfectly described by the Langmuir–Hinshelwood model. The combination of ultrasound and photocatalysis exhibited synergistic effect, which was found strongly dependent on the initial substrate concentration. A synergy factor of 1.15 was obtained for an initial substrate concentration of 10 mg L^{-1} but for 50 and 100 mg L^{-1}, the synergy factor increased significantly to 1.82 and 1.95, respectively. The synergy was mainly attributed to the advantages of ultrasound on the heterogeneous photocatalytic process.

Keywords: Phenol degradation; TiO_2-photocatalysis; Sonolysis; Sonophotocatalysis; Synergy

1. Introduction

The increase of industrial activities and intensive use of chemical substances such as aromatic hydrocarbons, chlorinated hydrocarbons, pesticides, dyes, dioxines and heavy metals have been contributed to environmental pollution with dramatic consequences in atmosphere, waters and soils [1,2]. Different methods of separation, degradation and elimination have been used in different polluting chemicals, which are generally present in wastewater coming out from the industrial sector [3]. The treatment of these pollutants can be efficiently achieved using advanced oxidation processes (AOPs) [4]. These processes are based on the production of hydroxyl radical (•OH) [4]. This species is extraordinarily reactive and attacks most organic molecules, with rate constants usually on the order of 10^6–10^9 mol L^{-1} s^{-1} [5].

* Corresponding author.

Heterogeneous photocatalysis over TiO_2 and sonolysis have independently attracted attention as AOPs for treating water [6–11]. Photoexcitation (with $\lambda < 390$ nm) of semiconducting TiO_2 promotes valence band electrons to the conduction band, thus leaving a reactive hole in the valence band [7]. Oxygen dissolved in the solution can scavenge excited electrons, forming superoxide ($O_2^{\bullet-}$) and its protonated form hydroperoxide ($HO_2^{\bullet}$) and, hence, limiting the electron-hole recombination [12]. Holes can react with adsorbed water molecules or hydroxides anions to form $^{\bullet}OH$ radicals, or can also be filled with an adsorbed organic donor [6,12]. Organic compounds may undergo oxidation directly at the hole or by means of $^{\bullet}OH$ radical [6]. On the other hand, the chemical effects of sonication arise from acoustic cavitation, namely the formation, growth and implosive collapse of bubbles in a liquid, which produces unusual chemical and physical environment [13]. The collapse of the bubbles induces localized extreme conditions (temperatures as high as 5,200 K and pressures higher than 500 atm within the bubble [14]). Under such conditions, molecules trapped in the bubble (water vapor, gases and vaporized solutes) can be brought to an excited state and dissociate [15]. As a result, reactive species such as $^{\bullet}OH$, $HO_2^{\bullet}$, $H^{\bullet}$ and O are created from H_2O and O_2 dissociation and their associate reactions in the bubble [15]. These active species can recombine, react with other gaseous species present in the cavity or diffuse out of the bubble into the bulk liquid medium to serve as oxidants [9]. Therefore, photocatalysis and ultrasonic irradiation can cause the degradation of organic pollutants with the same species, mainly $^{\bullet}OH$ radical.

Although photocatalysis with TiO_2 and sonolysis have been extensively investigated individually for the degradation of many organic compounds in aqueous media [16–24], their combination has become the focus of current research. Enhancement of the photocatalytic efficiency using low frequency ultrasound (20–100 kHz) has been widely investigated [25–30]. However, in spite of the notable performance of high-frequency ultrasound for the degradation of organics, only few reports have addressed the combination of photocatalysis and high frequency sonolysis. Théron et al. [25] reported that no synergy was observed between photocatalysis and 515 kHz ultrasound for the degradation of phenyltrifuoromethylketone. Moreover, sonophotocalysis with TiO_2 and 213 kHz showed a negative impact for the degradation of monocrotophos compared with photocatalysis alone [31]. On the other hand, Torres-Palma et al. [32,33] and Méndez-arriaga et al. [34] showed a significant synergy between photocatalysis and 300 kHz ultrasound for the degradation of bisphenol A and ibuprofen. Therefore, the synergy between photocatalysis and sonolysis toward the degradation of organic compounds remains controversial.

This work is a contribution to the study of the photocatalytic process and its coupling with high frequency sonolysis (600 kHz) in forced circulation loop process, using phenol as a substrate model. Phenol is one of the most common compounds found in the effluents of many industries such as petroleum refining and petrochemicals, pharmaceuticals, pesticides, paint and dye industries, organic chemicals manufacturing, etc. [35]. Its concentration has been reported in the range of trace quantities to thousands of milligrams per liter [36]. If present in even small quantities (of the order of a few ppm), phenol causes toxicity and foul odor to the water. It has been listed as a priority pollutant in the list of Environmental Protection Agency (EPA, USA) [35]. Therefore, there is more demand for applying AOPs for the removal of phenol from the effluent streams.

2. Materials and methods

2.1. Reagents

Phenol, supplied by Sigma-Aldrich (France), and titanium dioxide (TiO_2 P25), supplied by Degussa (France), were used as received.

2.2. Apparatus

Milli-Q water was used for the preparation of aqueous solutions and as component of the mobile phase in high performance liquid chromatography (HPLC) analysis. The experiments were carried out with 600 mL of air-equilibrated phenol solution at initial pH 6 in two connected systems, one under Suntest irradiation and the other one under sonication. The schematic diagram of the experimental setup is very similar to that showed by Torres-Palma et al. [32]. It consists of Pyrex glass vessel (200 mL) illuminated from the outside using a solar lamp CPS Suntest system (Atlas Gmbh, Germany) with a radiation intensity of 830 W m^{-2}. The lamp has a spectral distribution with about 0.5% of the emitted photons at wavelength shorter than 300 nm and about 7% between 300 and 400 nm. The emission spectrum between 400 and 800 nm follows the solar spectrum. The sonochemical reactor consists of a cylindrical water-jacketed glass (500 mL) cell to control the temperature. The ultrasonic waves emitted at 600 kHz and 70 W were delivered from the bottom through a piezoelectric disc (diameter 4 cm) fixed on Pyrex plate (diameter 5 cm). The temperature of the solution was kept at 20°C by circulating coolant through a jacket surrounding the cell. A peristaltic pump recirculated the solution from the sonochemical reactor to the photochemical reactor with a flow rate of 230 mL min^{-1}. The total solution volume (600 mL) was distributed as follows: 400 mL in the sonochemical reactor, 150 mL in the photochemical reactor and 50 mL in the connecting tubing. In this setup, we can test each system separately as well as the coupling photocatalysis/sonocatalysis. During the photocatalytic process, the sonicator was turned off, and stirring in the sonicator cell was performed. Bekkouche et al. [37] reported that the adsorption/desorption equilibrium of phenol on TiO_2 (P25) particles was attained after 40 min of treatment. Therefore, in photocatalysis or photocatalysis/sonocatalysis runs, the appropriate quantity of TiO_2 was added in the reacting mixture, and the suspension was left for 1 h with agitation in the dark to ensure a complete adsorption/desorption equilibrium of the pollutant. After that period, the Suntest lamp and/or the sonicator were turned on, and this was taken as time zero for the reaction.

Samples (1 mL) were withdrawn at different time intervals and filtrated with 0.2 μm Millipore filters (Whatman, France). The concentrations of phenol were then measured by HPLC (Waters® 510 HPLC). A Supelcosil C-18 column (internal diameter (i.d) = 4.6 mm, length = 25 cm) and a UV

detector set at 270 nm were used. The mobile phase, pumped at 1 mL min^{-1}, was composed of methanol (60%) and water (40%). All experiments were conducted at least in triplicate, and the data were averaged.

3. Results and discussion

3.1. Direct photolysis and TiO_2-photocatalytic degradation of phenol

Initial experiments were conducted to evaluate the efficiency of the phtocatalytic system using 1 g L^{-1} of TiO_2 toward the degradation of phenol (10 mg L^{-1}) in the batch-loop reactor. An addition control treatment with photolysis alone was included for the comparison. The volumetric flow rate of the solution was maintained at 230 mL min^{-1} for all experiments. The obtained results are shown in Fig. 1. This figure clearly indicates that the combined use of photolysis and TiO_2 had a significant higher phenol removal than the photolysis alone. After 300 min of treatment (5 h), phenol removal achieved 100% with the photocatalytic system, whereas only 50% was reached with photolysis alone. The initial degradation rate increased 10-fold when using photocatalysis system rather than photolysis (0.327 mg L^{-1} min^{-1} compared with 0.0323 mg L^{-1} min^{-1}). In all experimental conditions, phenol dark adsorption at equilibrium did not exceed 10% of its initial concentration.

The destruction of phenol in aqueous solution by photocatalysis (UV/TiO_2) or direct photolysis in batch system was investigated in several reports [38–42]. Grabowska et al. [43] delivered an interesting review on the mechanism of phenol photodegradation in the presence of TiO_2. Globally, the degradation of phenol by direct photolysis was reported by Chun et al. [38] and was attributed to the absorption of the UV light of wavelengths shorter than 400 nm. This range constitutes only ~8% of the solar spectrum of the modulator used in our experiments, which justified the lower photolytic conversion. Based on the intermediates detected during the TiO_2-photocatalytic degradation of phenol, it has been reported that •OH radicals attack the phenyl range, yielding catechol, resorcinol and hydroquinone, then the phenyl ranges in these compound break up to give malonic acid, then short-chain organic acids such as maleic, oxalic, acetic, formic and finally CO_2 [43]. Therefore, the principal reaction leading to phenol oxidation would be the one with •OH radical formed at the surface of the photocatalyst.

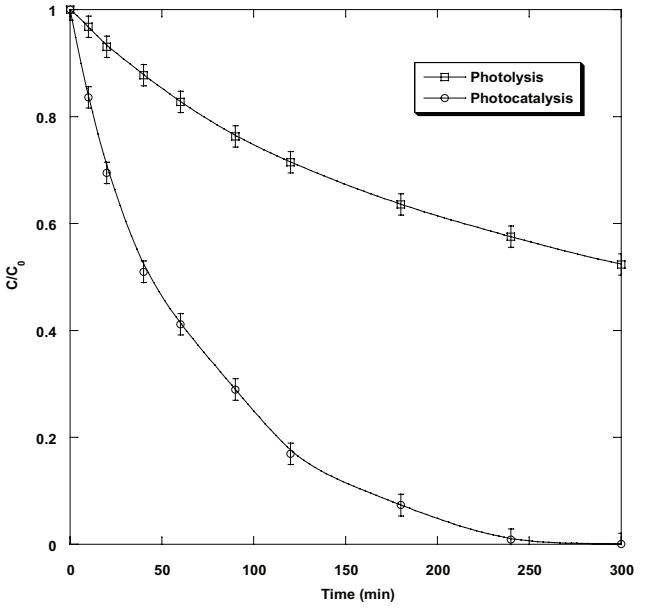

Fig. 1. Degradation kinetics of phenol with solar photolysis and photocatalysis in the batch-loop reactor (conditions – volume: 600 mL, TiO_2 loading: 1 g L^{-1}, initial substrate concentration: 10 mg L^{-1}, [TiO_2]: 1 g L^{-1}, volumetric flow rate: 230 mL min^{-1}, temperature: 20°C, pH: 6).

3.2. Effect of catalyst loading

The effect of TiO_2 concentration in the range of 0.01–2 g L^{-1} on the solar photocatalytic degradation of phenol was examined for an initial concentration of 10 mg L^{-1}. The results of the photocatalytic experiments are shown in Fig. 2. These results

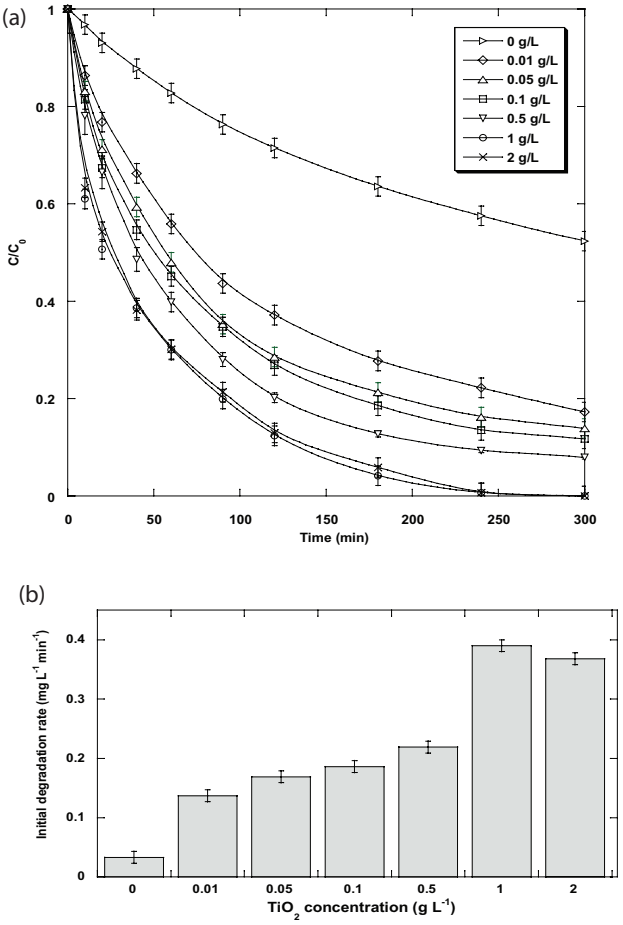

Fig. 2. Effect of catalyst loading on the photocatalytic degradation of phenol in the batch-loop reactor (conditions – volume: 600 mL, initial substrate concentration: 10 mg L^{-1}, [TiO_2]: 0.01–2 g L^{-1}, volumetric flow rate: 230 mL min^{-1}, temperature: 20°C, pH: 6): (a) degradation kinetics and (b) initial degradation rates vs. TiO_2 concentration.

clearly demonstrate that an increase in TiO_2 loading from 0.01 to 1 g L^{-1} resulted in significant increase in the degradation of phenol. The removal efficiency in the absence of TiO_2 (photolysis alone) was 36.4% after 3 h of treatment. This efficiency increased to 72.2%, 81.4%, 87.2% and 95.4% when TiO_2 was added at 0.01, 0.1, 0.5 and 1 g L^{-1}, respectively (Fig. 2(a)). In the presence of 0.01 mg L^{-1} of TiO_2, the initial degradation rate increased by factor of 3.84 compared with that obtained without catalyst and by factor of 5 and 10 when the TiO_2 concentration was increased to 0.1 and 1 g L^{-1}, respectively (Fig. 2(b)). However, an excess of TiO_2 above 1 g L^{-1} did not enhance further the degradation rate. Thus, a maximum degradation rate of phenol occurred at TiO_2 concentration of 1 g L^{-1}. These findings are in excellent agreement with those of Torres et al. [32] for bisphenol A, Berberidou et al. [30] for malachite green and Selli [26] for acid orange 8 dye.

The beneficial effect of TiO_2 in the range of 0.01–1 g L^{-1} toward phenol degradation was explained by the increase of the total photoactivated surface area (active sites) with increasing catalyst dosage, which increases the number of hydroxyl radical through interaction between light and TiO_2 particles. However, the deceleration in the degradation rate of phenol for catalyst concentration above 1 g L^{-1} is due to the aggregation of TiO_2 particles, which reduces the interfacial area between the reaction solution and the photocatalyst [27,32]. According to our results (Fig. 2), it can be concluded that this phenomenon starts to take place when the catalyst dosage exceeds 1 g L^{-1}. The increase in opacity and light scattering by the aggregated particles is another reason for the decrease in the degradation rate because it limits the absorption of light and this lowers the production of hydroxyl radicals [44]. The detrimental effect of TiO_2 above the optimum dose was largely reported in the literature [30,32,44–46].

3.3. Effect of initial phenol concentration

The effect of initial concentration of phenol on the solar photocatalytic process was studied by varying its concentration in the range of 1–100 mg L^{-1} using 1 g L^{-1} of TiO_2. Fig. 3 depicts the normalized-degradation kinetics for five initial concentrations (1, 5, 10, 50 and 100 mg L^{-1}). As can be seen, the removal efficiency decreased with increasing initial phenol concentration. Phenol elimination was completely achieved after 90 min of sonication for 1 mg L^{-1}, but the removal efficiency, at the same time, decreased to 85%, 71%, 47% and 38% when the initial concentration of phenol increased to 5, 10, 50 and 100 mg L^{-1}, respectively. However, for the same conditions, the destroyed amount of phenol, summarized in Table 1, showed an inverse trend. The destroyed amount increased by factor of 1.66, 5.53 and 9 when the initial concentration increased from 5 to 10, 50 and 100 mg L^{-1}, respectively. These results will be discussed and interpreted in the following section.

Fig. 4 displays the initial degradation rates of phenol (calculated from Fig. 3 as $\Delta C/\Delta t$ after few minutes of treatment) as function of its initial concentration. It was remarked that the higher the substrate concentration, the higher the initial degradation rate. However, a linear relationship was not observed, as expected, for a first-order kinetic law. These results are in accordance with those reported by several research studies for different pollutants [6,39,40]. The absence of linear

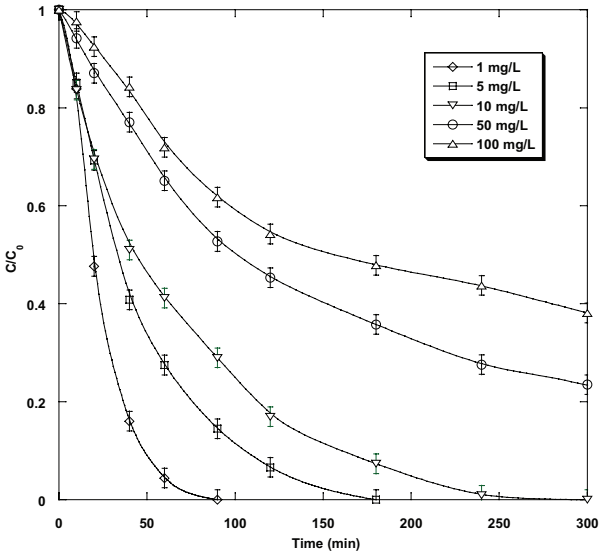

Fig. 3. Effect of initial substrate concentration on the photocatalytic degradation of phenol in the batch-loop reactor (conditions – volume: 600 mL, initial substrate concentration: 1–100 mg L^{-1}, [TiO_2]: 1 g L^{-1}, volumetric flow rate: 230 mL min^{-1}, temperature: 20°C, pH: 6).

Table 1
Destroyed amounts of phenol (calculated after 90 min of solar photocatalytic treatment) for various initial concentrations

Initial concentration (mg L^{-1})	Destroyed amounts (mg L^{-1})
1	1 ± 0.025
5	4.27 ± 0.106
10	7.10 ± 0.177
50	24.64 ± 0.616
100	38.24 ± 0.951

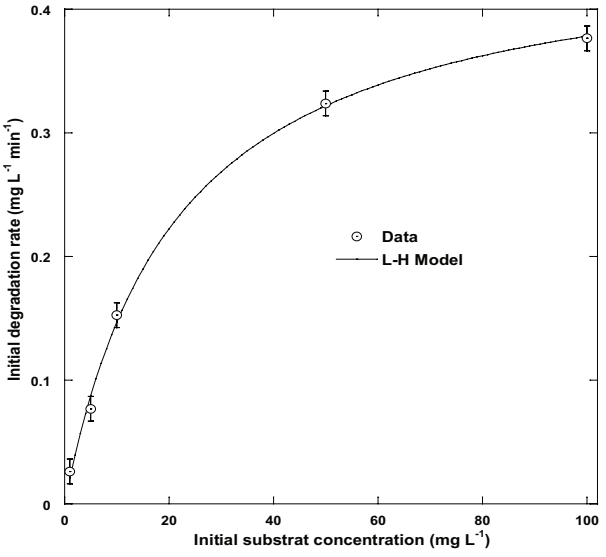

Fig. 4. Variation of the initial degradation rate of phenol (data and fit) vs. initial concentration, for the same condition as in Fig. 3.

relationship between the initial degradation rate and the initial phenol concentration clearly indicates that solar photocatalytic degradation of phenol cannot be associated with first-order kinetics. A heterogeneous kinetics model based on Langmuir–Hinshelwood (L–H) equation (Eq. (1)) [6,43] was applied to fit the experimental data. Even if this kinetics model is used to assume automatically that reactions take place at the surface of the catalyst particles, most authors agree that, with minor variations, the expression for the rate of photocatalytic degradation and mineralization of organic substrates with irradiated TiO_2 follows the L–H law whatever the reactions take place on the catalyst surface or in the fluid phase [6].

$$r = \frac{k_r K C_0}{1 + K C_0} \quad (1)$$

In Eq. (1), r is the initial degradation rate (mg L^{-1} min^{-1}); k_r is the reaction rate constant (mg L^{-1} min^{-1}); K is the L–H adsorption equilibrium constant (L mg^{-1}) and C_0 is the initial concentration of phenol (mg L^{-1}). The model parameters were determined by non-linear curve-fitting method using KaleidaGraph© software. The obtained values are k_r = 0.4584 mg L^{-1} min^{-1} and K = 0.04715 L mg^{-1}, and the corresponding theoretical curve was superimposed on the experimental data points (Fig. 4). It was clearly seen that the L–H kinetic model perfectly described the photocatalytic degradation rate of phenol, signifying that phenol degradation rate is not only related to its concentration but also to the available reaction sites at catalyst surface, which control the local concentration of •OH radicals. Thus, with increasing initial pollutant concentration in the bulk solution, more and more phenol molecules will be available at the catalyst surface, and this increases the probability of •OH radical attack on phenol molecules, leading to an increase in the degradation rate as observed in Fig. 4. However, this is valid for the studied range of initial concentration (1–100 mg L^{-1}), because a continuous increase in initial substrate concentration does not necessarily imply a continual increase in the degradation rate. At a certain point of high initial substrate concentrations, the catalyst surface will be saturated, and the degradation rate becomes steady as found by Malato et al. [6].

3.4. Effect of coupling photocatalysis with high frequency sonolysis

Before studying the combination effect of photocatalysis and sonolysis, it is of interest to investigate firstly the action of ultrasound and ultrasound/TiO_2 processes separately on the degradation of phenol in the forced circulation loop system. Fig. 5 shows the results of the sonochemical degradation (600 kHz, 70 W) of 10 mg L^{-1} of phenol in the absence and presence of various concentrations of TiO_2. As seen, ultrasound alone degraded phenol. During sonolysis, volatile substrates will be pyrolyzed in the bubble by the high core temperature whereas non-volatile substrates will be oxidized by hydroxyl radicals at the bubble-liquid interface and in the bulk liquid solution [47]. Extensive works on the sonolytic degradation of phenol were conducted by the research group of Prof. Pétrier [11,16,47]. They established that phenol cannot enter the bubbles but it is degraded by hydroxyl radical

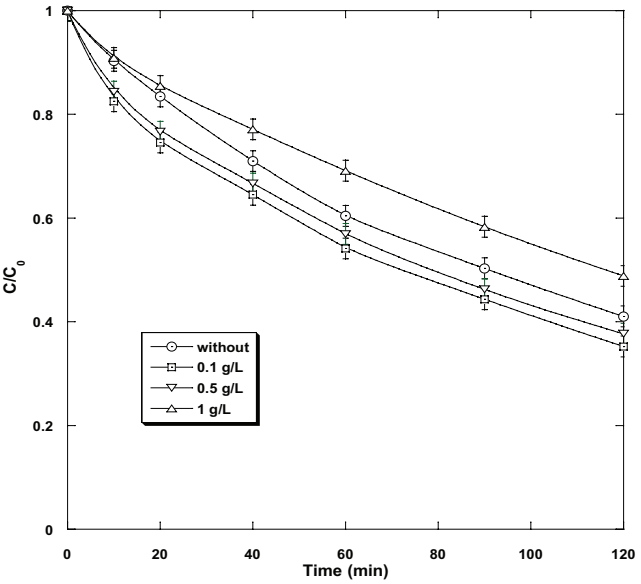

Fig. 5. Effect of TiO_2 loading on the sonochemical degradation of phenol in the batch-loop reactor (conditions – volume: 600 mL, initial substrate concentration: 10 mg L^{-1}, [TiO_2]: 0.1–1 g L^{-1}, volumetric flow rate: 230 mL min^{-1}, temperature: 20°C, pH: 6, frequency: 600 kHz, power: 70 W).

attack at the cavitation bubbles interface (conclusion based on the identification of phenol degradation by-products). It should be mentioned that some oxygen and nitrogen-active species, such as $HO_2^{\bullet}$, $NO_2^{\bullet}$ and $NO_3^{\bullet}$, may be formed from O_2 and N_2 sonolysis and their associate reactions in the bubble under ultrasound action of aerated solution [48]. However, in addition to their lower activities compared with that of •OH [49–51], the concentration of these species is very low to be involved in the degradation mechanism [48].

Fig. 5 shows that the presence of catalyst at 0.1 g L^{-1} in the sonicating medium enhanced slightly the degradation of the pollutant. This is due to the TiO_2 particles, providing extra nuclei for bubble formation [52]. However, the observed positive effect was reduced and disappeared when using 0.5 and 1 g L^{-1} of TiO_2. This phenomenon was also reported by Berberidou et al. [30] and Torres et al. [32] and was mainly attributed to the attenuation of ultrasound waves by the catalyst particles, which reduces the penetration of ultrasonic waves in the solution. Overall, as the positive and negative effects of TiO_2 on the sonolytic degradation of phenol are marginals (~7% for each one), the optimum amount of TiO_2 obtained for the photocatalytic reaction (1 g L^{-1}) was maintained for the sonophotocatatytic experiments.

Fig. 6 shows the degradation-time profiles of phenol for 2 h of treatment under ultrasound, ultrasound/TiO_2 (sonocatalysis), photocatalysis and sonophotocatalysis. It is clearly seen from this figure that the degradation rate follows the following order: sonocatalysis < sonolysis < photocatalysis < sonophotocatalysis, and the beneficial effect of sonophotocatalysis treatment on phenol abatement is very remarkable. After 2 h, ~91% of phenol was degraded using sonophotocatalysis whereas 82% was eliminated with photocatalysis, 58% with ultrasound alone and only 51% with sonocatalysis. More interestingly, a synergy of 1.15 was

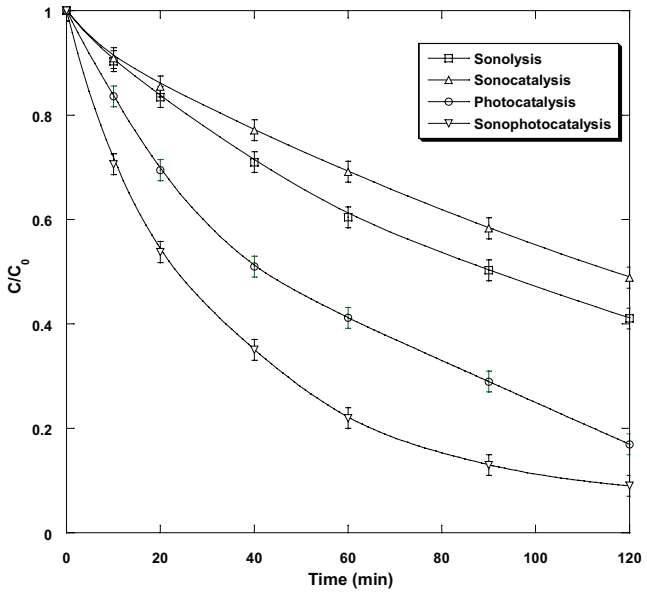

Fig. 6. Degradation kinetics of phenol with photocatalysis, sonolysis and sonophotocatalysis in the batch-loop system (conditions – volume: 600 mL, initial substrate concentration: 10 mg L^{-1}, flow rate: 230 mL min^{-1}, temperature: 20°C, pH: 6, frequency: 600 kHz, power: 70 W).

observed when combining ultrasound with photocatalysis using 1 g L^{-1} of TiO_2. This result is in good agreement with that reported by Torres et al. [56] at 300 kHz and 80 W. The synergy, *S*, was calculated using the following equation [31]:

$$S = \frac{r_{\text{sonophotocatalysis}}}{r_{\text{phptocatalysis}} + r_{\text{sonocatalysis}}} \quad (2)$$

where $r_{\text{sonophotocatalysis}}$, $r_{\text{photocatalysis}}$ and $r_{\text{sonocatalysis}}$ are the degradation rates of phenol with sonophotocatalysis, photocatalysis and sonocatalysis, respectively.

In order to explore the dependence of the synergy *S* to the initial pollutant concentration, sonocatalytic and sonophotocaralytic experiments, with 1 g L^{-1} of TiO_2, were conducted for various initial phenol concentrations in the range of 1–100 mg L^{-1}. Fig. 7 shows the variation of initial degradation rate as function of initial phenol concentration for the three processes (sonocatalysis, photocatalysis and sonophotocatalysis). The corresponding effect of initial substrate concentration on the synergy *S* is shown in Table 2. From Fig. 7, it was obviously seen that the sonocatalytic as well as sonophotocatalytic degradation didn't follow first-order kinetic law as there is no linear relationships between the initial degradation rate and the initial concentration. Additionally, for all initial concentrations, the order sonocatalysis < photocatalysis < sonophotocatalysis toward the degradation of phenol was observed. More interestingly, the beneficial effect of the combined treatment is very remarkable at high levels of initial substrate concentration. For example, the initial degradation rate obtained by sonophotocatalysis at 10 mg L^{-1} is as much as about 3.3 and 1.57 times greater than those obtained by sonocatalysis and photocatalysis,

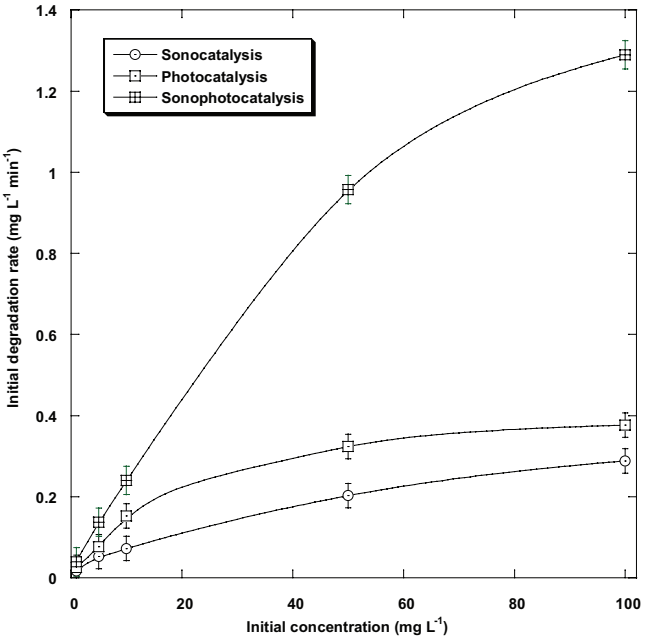

Fig. 7. Effect of initial substrate concentration of the degradation rate of phenol with photocatalysis, sonocatalysis and sonophotocatalysis in the batch-loop system (conditions – volume: 600 mL, initial substrate concentration: 1–100 mg L^{-1}, flow rate: 230 mL min^{-1}, temperature: 20°C, pH: 6, frequency: 600 kHz, power: 70 W).

Table 2
Synergy between photocatalysis and sonocatalysis with respect to the initial substrate concentration

Initial concentration (mg L^{-1})	Synergy (*S*)
1	0.91 ± 0.022
5	1.06 ± 0.026
10	1.15 ± 0.028
50	1.82 ± 0.045
100	1.95 ± 0.048

respectively. However, for 100 mg L^{-1} of phenol, sonophotocatalysis yielded an initial degradation rate, which is about ~4.5 and 3.4 times larger than those calculated for sonocatalysis and photocatalysis, respectively. Correspondingly, the synergy factor (*S*) increased with increasing initial substrate concentration. It was more important at 50 and 100 mg L^{-1}, i.e., 1.82 and 1.95, respectively. At 5 mg L^{-1} the combination effect is additive whereas at 1 mg L^{-1} photocatalysis was negatively affected by the presence of ultrasound at 600 kHz. To the best of our knowledge, the obtained synergy-dependence of the initial substrate concentration was never addressed previously.

Photocatalysis and sonocatalysis, the two processes under investigation contribute to the production of •OH as a dominant free radical, which is responsible for increasing the rates of reaction. Taking into account that TiO_2 particles at 1 g L^{-1} did not enhance the ultrasonic degradation of phenol (Fig. 6), the obtained synergy between photocatalysis and

sonocatalysis toward the degradation of phenol was mainly attributed to the advantages of cavitation on heterogamous photocatalysis, as listed below:

- In addition to the production of •OH radical, ultrasound generates a significant amount of H_2O_2 from the radicals' recombination at the bubbles interface [53]. Its concentration, varied from 1 to several μM min^{-1} [32,47,54,55]. The ultrasonically yielded H_2O_2 promotes the production of additional •OH radicals in the reacting medium through two ways: (i) by direct UV-photolytic decomposition (Eq. (3)) [56] and (ii) by reduction of electron-hole recombination as H_2O_2 is better electron accepter than O_2 (Eq. (4)) [57].

$$H_2O_2 \xrightarrow{hv} 2^{\bullet}OH \quad (3)$$

$$TiO_2(e^-) + H_2O_2 \rightarrow TiO_2 + {}^{\bullet}OH + {}^{-}OH \quad (4)$$

- Ultrasound increases the catalyst surface area due to its de-aggregation, fragmentation and pitting actions on the photocatalyst particles [58]. This enhanced the performance of the photocatalytic process. In fact, Chave et al. [59] have evidenced that the catalytic activity of TiO_2-catalyst is enhanced by high frequency ultrasound due to the strong dispersion effect. It was shown that at 360 kHz the main size of TiO_2 aggregates in aqueous solutions decreases from ~50 to ~1 μm even after short-time ultrasound treatment [59].
- Cleaning and sweeping of the TiO_2 surface due to acoustic microstreaming allows more available active sites at any given time.
- Mass transport of the reactants and products is increased at the catalyst surface and in the solution, due to the facilitated transport by shockwave propagation.

4. Conclusion

The degradation of phenol by solar TiO_2-phtocatalysis, sonocatalysis and sonophotocatalysis was investigated in forced circulation loop process that couples a photochemical reactor with sonochemical reactor operating at high frequency ultrasound (600 kHz and 70 W). It was found that the photocatalytic reaction rate is significantly influenced by the operating parameters, i.e., pollutant concentration and TiO_2 loading. The degradation rate was more efficient when coupling ultrasound with TiO_2-photocatalysis. Sonophotocatalysis in the batch-loop mode exhibited a synergistic effect, which was mainly attributed to the effects of ultrasound on the photocatalytic process. This process should be a promising technique for the degradation of organic pollutants in water. However, further efforts should be carried out to investigate the performance of this technology under various real matrices.

Acknowledgment

The financial support by the Ministry of Higher Education and Scientific Research of Algeria (project No. A16N01UN230120130010) is greatly acknowledged.

References

[1] K. Wark, C.F. Warner, W.T. Davis, Air Pollution: Its Origin and Control, Addison-Wesley, USA, 1998.
[2] B.M. Huang, I.K. Iskandar, Soils and Groundwater Pollution and Remediation: Asia, Africa and Oceania, CRC Press LLC, USA, 1999.
[3] A.D. Patwardhan, Industrial Waste Water Treatment, Prentice-Hall of India Private Limited, New Delhi, 2008.
[4] J.L. Wang, L.J. Xu, Advanced oxidation processes for wastewater treatment: formation of hydroxyl radical and application, Crit. Rev. Environ. Sci. Technol., 42 (2012) 251–325.
[5] M.A. Tarr, Chemical Degradation Methods for Wastes and Pollutants, Marcel Dekker, Inc., New York, 2003.
[6] S. Malato, P. Fernandez-Ibanez, M.I. Maldonado, J. Blanco, W. Gernjak, Decontamination and disinfection of water by solar photocatalysis: recent overview and trends, Catal. Today, 147 (2009) 1–59.
[7] J.-M. Herrmann, Heterogeneous photocatalysis: fundamentals and applications to the removal of various types of aqueous pollutants, Catal. Today, 53 (1999) 115–129.
[8] C.S. Truchi, D.F. Ollis, Photocatalytic degradation of organic water contaminants: mechanism involving hydroxyl radical attack, J. Catal., 122 (1990) 178–192.
[9] Y.G. Adewuyi, Sonochemistry: environmental science and engineering applications, Ind. Eng. Chem. Res., 40 (2001) 4681–4715.
[10] M.R. Hoffmann, I. Hua, R. Hochemer, Application of ultrasonic irradiation for the degradation of chemical contaminants in water, Ultrason. Sonochem., 3 (1996) S163–S172.
[11] C. Pétrier, D. Casadonte, The sonochemical degradation of aromatic and chloroaromatic contaminants, Adv. Sonochem., 6 (2001) 91–109.
[12] K. Hashimoto, H. Irie, A. Fujishima, TiO_2 photocatalysis: a historical overview and future prospects, Jpn. J. Appl. Phys., Part 1, 44 (2005) 269–8285.
[13] K.S. Suslick, Y. Didenko, M.M. Fang, T. Hyeon, K.J. Kolbeck, W.B. McNamara, M.M. Mdleleni, M.M. Wong, Acoustic cavitation and its chemical consequences, Phil. Trans. Roy. Soc. Lond. A, 357 (1999) 335–353.
[14] K.S. Suslick, D.J. Flannigan, Inside a collapsing bubble: sonoluminescence and the conditions during cavitation, Annu. Rev. Phys. Chem., 59 (2008) 659–683.
[15] L.H. Thompson, L.K. Doraiswamy, Sonochemistry: science and engineering, Ind. Eng. Chem. Res., 38 (1999) 1215–1249.
[16] C. Pétrier, M.F. Lamy, A. Francony, A. Benahcen, B. David, Sonochemical degradation of phenol in dilute aqueous solutions: comparison of the reaction rates at 20 and 487 kHz, J. Phys. Chem., 9 (1994) 10514–10520.
[17] S. Merouani, O. Hamdaoui, F. Saoudi, M. Chiha, Sonochemical degradation of Rhodamine B in aqueous phase: effects of additives, Chem. Eng. J., 158 (2010) 550–557.
[18] F. Méndez-Arriaga, R.A. Torres-Palma, C. Pétrier, S. Esplugas, Ultrasonic treatment of water contaminated with ibuprofen, Water Res., 42 (2008) 4243–4248.
[19] M. Chiha, O. Hamdaoui, S. Baup, N. Gondrexon, Sonolytic degradation of endocrine disrupting chemical 4-cumylphenol in water, Ultrason. Sonochem., 18 (2011) 943–950.
[20] Y.-Q. Gao, N.-Y. Gao, Y. Deng, J.-S. Gu, Y.-L. Gu, D. Zhang, Factor affecting sonolytic degradation of sulfamethazine in water, Ultrason. Sonochem., 20 (2013) 1401–1407.
[21] H. Lachheb, E. Puzenat, A. Houas, M. Ksibi, E. Elaloui, C. Guillard, J.-M. Herrmann, Photocatalytic degradation of various types of dyes (Alizarin S, Crocein Orange G, Methyl Red, Congo Red, Methylene Blue) in water by UV-irradiated titania, App. Catal., B, 39 (2002) 75–90.
[22] F. Méndez-Arriaga, S. Espugas, J. Giménez, Photocatalytic degradation of non-steroidal anti-inflamatory drugs with TiO_2 and simulated solar irradiation, Water Res., 42 (2008) 585–594.
[23] F. Méndez-Arriaga, M.I. Maldonado, J. Giménez, S. Espugas, S. Malato, Abatement of ibuprofen by solar photocatalysis process: enhancement and scale up, Catal. Today, 144 (2009) 112–116.

[24] E.M. Rodriguez, G. Marquez, M. Tena, P.M. Alvarez, F.J. Beltran, Determination of main species involved in the first steps of TiO_2 photocatalytic degradation of organics with the use of scavengers: the case of ofloxacin, App. Catal., B, 178 (2015) 44–53.
[25] P. Théron, P. Pichat, C. Guillard, C. Pétrier, T. Chopinc, Degradation of phenyltrifuoromethylketone in water by separate or simultaneous use of TiO_2 photocatalysis and 30 or 515 kHz ultrasound, Phys. Chem. Chem. Phys., 1 (1999) 4663–4668.
[26] E. Selli, Synergistic effect of sonolysis combined with photocatalysis in the degradation of an azo dye, Phys. Chem. Chem. Phys., 4 (2002) 6123–6128.
[27] T. An, H. Gu, Y Xiong, W. chen, X. Zhu, G. Sheng, J. Fu, Decolourization and COD removal from reactive dye-containing wastewater using sonophotocatalytic technology, J. Chem. Technol. Biotechnol., 78 (2003) 1142–1148.
[28] F. Ahmedchekkat, M.S. Medjram, M. Chiha, A.M.A. Al-bsoul, Sonophotocatalytic degradation of Rhodamine B using a novel reactor geometry: effect of operating paramaters, Chem. Eng. J., 178 (2011) 144–251.
[29] C.D. Wu, J.Y. Zhang, Y. Wu, G.Z. Wu, Degradation of phenol in water by the combination of sonolysis and photocatalysis, Desal. Wat. Treat., 52 (2014) 1911–1918.
[30] C. Berberidou, I. Poulios, N.P. Xekoukoulotakis, D. Mantzavinos, Sonolytic, photocatalytic and sonophotocatalytic degradation of Malachite Green in aqueous solutions, Appl. Catal., B, 74 (2007) 63–72.
[31] J. Madhavan, P.S. Sathish Kumar, S. Anandan, F. Grieser, M. Ashokkumar, Sonophotocatalytic degradation of monocrotphpos using TiO_2 and Fe^{3+}, J. Hazard. Mater., 177 (2009) 944–949.
[32] R.A. Torres-Palma, J.I. Nieto, E. Combet, C. Pétrier, C. Pulgarin, Influence of TiO_2 concentration on the synergistic effect between photocatalysis and high-frequency ultrasound for organic pollutant mineralization in water, Appl. Catal., B, 80 (2008) 168–175.
[33] R.A. Torres-Palma, J.I. Nieto, E. Combet, C. Pétrier, C. Pulgarin, An innovative ultrasound, Fe^{2+} and TiO_2 photoassisted process for bisphenol a mineralization, Water Res., 44 (2010) 2245–2252.
[34] F. Méndez-Arriaga, R.A. Torres-Palma, C. Pétrier, S. Esplugas, J. Gimenez, C. Pulgarin, Mineralization enhancement of a recalcitrant pharmaceutical pollutant in water by advanced oxidation hybrid processes, Water Res., 43 (2009) 3984–3991.
[35] N.N. Mahamuni, A.B. Pandit, Effect of additives on ultrasonic degradation of phenol, Ultrason. Sonochem., 13 (2006) 165–174.
[36] J. Wu, K.E. Taylor, J.K. Bewtra, N. Biswas, Optimization of the reaction conditions for enzymatic removal of phenol from wastewater in the presence of polyethylene glycol, Water Res., 27 (1993) 1701–1706.
[37] S. Bekkouche, M. Bouhelassa, N. Hadj Salah, F.Z. Meghlaou, Study of adsorption of phenol on titanium oxide (TiO_2), Desalination, 166 (2004) 355–362.
[38] H. Chun, W. Yizhong, T. Hongxiao, Destruction of phenol aqueous solution by photocatalysis or direct photolysis, Chemosphere, 41 (2000) 1205–1209.
[39] R. Qiu, L. Song, Y. Mo, D. Zhang, E. Brewer, Visible light induced photocatalytic degradation of phenol by polymer-modified semiconductors: study of the influencing factors and the kinetics, React. Kinet. Catal. Lett., 97 (2008) 183–189.
[40] A. Sobczynski, L. Duczmal, W. Zmudzinski, Phenol destruction by photocatalysis on TiO_2: an attempt to solve the reaction mechanism, J. Mol. Catal. A: Chem., 213 (2004) 225–230.
[41] Z. Guo, R. Ma, G. Li, Degradation of phenol by nanomaterial TiO_2 in wastewater, Chem. Eng. J., 119 (2006) 55–59.
[42] P. Gorska, A. Zaleska, J. Hupka, Photodegradation of phenol by UV/TiO_2 and Vis/N, C-TiO_2 processes: comparative mechanistic and kinetics studies, Sep. Purif. Methods, 68 (2009) 90–96.
[43] E. Grabowska, J. Reszczynska, A. Zaleska, Mechanism of phenol photodegradation in the presence of pure and modified-TiO_2: a review, Water. Res., 46 (2012) 5453–5471.
[44] N. San, A. Hatipoglu, G. Kocturk, Z. Cinar, Photocatalytic degradation of 4-nitrophenol in aqueous TiO_2 suspensions: theoretical prediction of the intermediates, J. Photochem. Photobiol., A, 146 (2002) 189–197.
[45] P. Saritha, C. Aparna, V. Himabindu, Y. Anjaneyulu, Comparison of various advanced oxidation processes for the degradation of 4-chloro-2 nitrophenol, J. Hazard. Mater., 149 (2007) 609–614.
[46] Q. Hu, C. Zhang, Z. Wang, Y. Chen, K. Mao, X. Zhang, Y. Xiong, M. Zhu, Photodegradation of methyl tert-butyl ether (MTBE) by UV/H_2O_2 and UV/TiO_2, J. Hazard. Mater., 154 (2008) 795–803.
[47] C. Pétrier, A. Francony, Ultrasonic wastewater treatment: incidence of ultrasonic frequency on the rate of phenol and carbon tetrachloride degradation, Ultrason. Sonochem., 4 (1997) 295–300.
[48] H. Ferkous, S. Merouani, O. Hamdaoui, Y. Rezgui, M. Guemini, Comprehensive experimental and numerical investigations of the effect of frequency and acoustic intensity on the sonolytic degradation of naphthol blue black in water, Ultrason. Sonochem., 26 (2015) 30–39.
[49] B.H.J. Bielski, D.E. Cabelli, R.L. Arudi, A.B. Ross, Reactivity of $HO_2/O_2^{\bullet-}$ radicals in aqueous solution, J. Phys. Chem. Ref. Data, 14 (1985) 1041–1100.
[50] G.V. Buxton, C.L. Greenstock, W.P. Helman, A.B. Ross, Critical review of rate constants for reactions of hydrated electrons, hydrogen atoms and hydroxyl radicals ($^{\bullet}OH/^{\bullet}O^{-}$) in aqueous solution, J. Phys. Chem. Ref. Data, 17 (1988) 513–886.
[51] P. Neta, R.E. Huie, A.B. Ross, Rate constants for reactions of inorganic radicals in aqueous solution, 17 (1988) 1027–1284.
[52] M. Kubo, K. Matsuoka, A. Takahashi, N. Shibasaki-Kitakawa, T. Yonemoto, Kinetics of ultrasonic degradation of phenol in the presence of TiO_2 particles, Ultrason. Sonochem., 12 (2005) 263–269.
[53] P. Kanthale, F. Ashokkumar, F. Grieser, Sonoluminescence, sonochemistry (H_2O_2 yield) and bubble dynamics: frequency and power effects, Ultrason. Sonochem., 15 (2008) 143–150.
[54] R. Pflieger, T. Chave, G. Vite, L. Jouve, S.I. Nikitenko, Effect of operational conditions on sonoluminescence and kinetics of H_2O_2 formation during the sonolysis of water in the presence of Ar/O_2 gas mixture, Ultrason. Sonochem., 26 (2015) 169–175.
[55] H. Ferkous, O. Hamdaoui, S. Merouani, Sonochemical degradation of naphthol blue black in water: effect of operating parameters, Ultrason. Sonochem., 26 (2015) 30–39.
[56] R.A. Torres-Palma, C. Pétrier, E. Combet, F. Moulet, C. Pulgarin, Bisphenol A mineralization by integrated ultrasound-UV-iron (II) treatment, Environ. Sci. Technol., 41 (2007) 297–302.
[57] P. Pattanaik, M.K. Sahoo, TiO_2 photocatalysis: progress from fundamentals to modification technology, Desal. Wat. Treat., 52 (2014) 6567–6590.
[58] M. Siddique, R. Khan, A.F. Khan, R. Farooq, Improved photocatalytic activity of TiO_2 coupling ultrasound for reactive blue 19 degradation, J. Chem. Soc. Pak., 3 (2014) 37–43.
[59] T. Chave, N.M. Navarro, P. Pochon, N. Perkas, A. Gedanken, S.I. Nikitenko, Sonocatalytic degradation of oxalic acid in the presence of oxygen and Pt/TiO_2, Catal. Today, 241 (2015) 55–62.